Received: 4 January 2018 | Revised: 19 July 2018 | Accepted: 24 July 2018

DOI: 10.1111/geb.12824

RESEARCH PAPER

WILEY Global Ecology and Biogeography A Journal of Macroecology

The colour of environmental fluctuations associated with terrestrial animal population dynamics

David Gilljam[1] | Jonas Knape[2] | Andreas Lindén[3] | Marianne Mugabo[4] | Steven M. Sait[4] | Mike S. Fowler[1,5]

[1]Dynamic Ecology Group, Department of Biosciences, College of Science, Swansea University, Swansea, United Kingdom

[2]Department of Ecology, Swedish University of Agricultural Sciences, Uppsala, Sweden

[3]Novia University of Applied Sciences, Ekenäs, Finland

[4]Faculty of Biological Sciences, School of Biology, University of Leeds, Leeds, United Kingdom

[5]Population Ecology Group, Institut Mediterrani d'Estudis Avançats (UIB-CSIC), Esporles, Spain

***Correspondence**
David Gilljam, Dynamic Ecology Group, Department of Biosciences, College of Science, Swansea University, Swansea SA2 8PP, United Kingdom.
Email: d.a.gilljam@swansea.ac.uk

Funding information
Natural Environment Research Council, Grant/Award Number: NE/N00213X/1 and NE/N002849/1

Abstract

Aim: The temporal structure (colour) of environmental variation influences population fluctuations, extinction risk and community stability. However, it is unclear whether environmental covariates linked to population fluctuations are distinguishable from a purely random process (white noise). We aimed to estimate colour coefficients and relative support for three models commonly representing coloured stochastic processes, in environmental series linked to terrestrial animal population fluctuations.

Location: North America and Eurasia.

Time period: 1901–2002.

Major taxa studied: Birds, insects and mammals.

Methods: We analysed multiple abiotic environmental covariates, comparing point estimates and confidence intervals of temporal structure in competing models fitted using white noise, autoregressive [AR(1)] and $1/f$ processes in the time domain and the frequency domain (where time series were analysed after decomposition into different sinusoidal frequencies and their relative powers). All animal time series were sampled annually for ≤ 50 years, potentially inflating type II errors. We also considered 101-year series of matched environmental covariates, performing a statistical power analysis evaluating our ability to draw robust conclusions.

Results: Temperature-related variables were associated with the largest fraction of population fluctuations. Ninety-three per cent of shorter environmental series were indistinguishable from white noise, limited by time-series length and associated with wide confidence intervals. The longer environmental series analysed in the time domain offered sufficiently high statistical power to identify correctly colour estimates ≥ |0.27|, indicating that 20% of series were best described by a slightly reddened noise process.

Main conclusions: Focusing on the short time-scales typically available for ecologists, most environmental variables associated with terrestrial animal population fluctuations are best characterized by white noise processes, although type II errors are common. The correct detection of intermediately coloured noise with power 0.8 requires ≥ 16 data points in the time domain or ≥ 47 points in the frequency domain. Over longer time-scales, where type II errors are less likely, one-fifth of populations are associated with coloured (often reddened) variables.

KEYWORDS
climate, environmental forcing, environmental variation, fluctuations, frequency domain, population dynamics, spectral colour, time domain, time series

1 | INTRODUCTION

A major issue in population biology concerns how the colour of environmental variation interacts with population dynamics to drive observed patterns of population fluctuations (e.g., Dillon et al., 2016; Halley, 1996; Ruokolainen, Lindén, Kaitala, & Fowler, 2009; Steele, 1985). Here, colour refers to the temporal and/or spatial structure of variation that describes system dynamics. Analogous to the visible light spectrum, low frequencies (slow fluctuations) dominate in red environments, high frequencies (rapid fluctuations) dominate in blue environments, while no frequencies are dominant in white, purely random environments (Halley, 1996). Environmental colour is predicted to interact with population demographic processes, such as survival, reproductive and developmental rates, stage structure or age structure, the intensity of intra- and interspecific competition and the shape and strength of density dependence (Ruokolainen, Lindén, et al., 2009). These interactions will modify the size of and correlation between the environment and population fluctuations, affecting ecological factors such as the extinction risk of single species populations (Cuddington & Yodzis, 1999; Inchausti & Halley, 2003; Pimm & Redfearn, 1988; but see Fowler & Ruokolainen, 2013a) and in multispecies communities and spatially structured systems (Fowler & Ruokolainen, 2013b; Gonzalez & de Feo, 2007; Gudmundson, Eklöf, & Wennergren, 2015; Lögdberg & Wennergren, 2012; Ruokolainen, Ranta, Kaitala, & Fowler, 2009). The interaction between environmental colour and population demographic processes will also modify species interactions (e.g., prey–predator, competition, host–parasites) and ecosystem stability and function (Fowler & Ruokolainen, 2013a, 2013b; Greenman & Benton, 2005; Gudmundson et al., 2015; Inchausti & Halley, 2003; Lögdberg & Wennergren, 2012; Ripa & Heino, 1999; Ripa & Ives, 2003; Roughgarden, 1975; Ruokolainen & Fowler, 2008; Ruokolainen, Fowler, & Ranta, 2007; Ruokolainen, Ranta, et al., 2009). Furthermore, the response of species to coloured environmental variation depends on the time-scale considered, the extent to which it coincides with the life cycle of an organism and the particular life-history traits that are affected by environmental change (Heino & Sabadell, 2003). Additionally, environmental variables in reddened environments imply consecutive periods (days, weeks, years) of favourable or unfavourable conditions, which may decrease or increase extinction risk, respectively (Schwager, Johst, & Jeltsch, 2006). Populations with undercompensating growth tend to respond slowly to environmental changes; therefore, fluctuations in density are amplified under red environmental variation, which increases their extinction risk (Roughgarden, 1975). Large-scale changes in climate variables associated with the El Niño Southern Oscillation (SO) or North Atlantic Oscillation (NAO) indices, which may encapsulate overall fluctuations in local environmental fluctuations (Post & Forchhammer, 2002), also impact on the dynamics of populations (Coulson et al., 2001; Hallett et al., 2004).

One of the main challenges when studying the impact of coloured environmental variation on population dynamics is the accuracy of colour coefficients estimated from environmental time series. Autocorrelated processes have been observed and studied in many different fields, and the terminologies and methodologies used for their description and detection vary across disciplines. For example, within the geophysical and climatological sciences, variability correlated at all time-scales is often referred to as long-term persistence (e.g., Halley, 2009; Rybski et al., 2006) or the 'Hurst effect' (Hurst, 1951; reviewed by O'Connell et al., 2016), where strong long-term persistence characterizes a domination of low-frequency (slow or reddened) fluctuations. In ecology, two methods are commonly used to generate and/or statistically model coloured stochastic processes; autoregressive [AR(k), where k gives the order of the process, most frequently performed in the time domain] or sinusoidal [$1/f^{\beta}$, where β is the spectral exponent, describing the linear relationship between log(signal power) and log(frequency) in the frequency domain, referred to hereafter as $1/f$ processes]. Analysis in the time domain investigates correlations between values of the series at different times, whereas analysis in the frequency domain is a standardized method for decomposing the overall variance of a time series into contributions from different frequencies (e.g., Chatfield, 1996; Dillon et al., 2016). These processes differ in some respects; for example, the variance grows continuously with observation time in a $1/f$ process, whereas variance growth will eventually cease in an autoregressive process (Halley, 2005). The methodology used and the time-scales at which observations of the focal variable are made will impact our perception of the true variability of, for example, climate covariates (Király & Jánosi, 2002; Ruokolainen, Lindén, et al., 2009). For example, in a white noise process, the total variance is independent of observation sampling frequency but scales linearly with the amount of sample aggregation, whereas in a coloured process the total variance depends on time-series length, sample timing and aggregation (Halley, 2007). In $1/f$ models, low sampling frequency can result in a systematic 'whitening' (or 'aliasing') of the power spectrum, which yields estimates closer to zero compared with the true colour (Kirchner, 2005). However, aliasing can be offset by sampling aggregation (e.g., seasonal averages calculated from daily samples; Halley, 2007, 2009; Kirchner, 2005). The detection of processes other than white noise (avoiding type II statistical errors) is especially difficult when time series are short and the true colour is close to zero (Gerrodette et al., 1987; Miramontes & Rohani, 2002; Pimm & Redfearn, 1988), which has led to the development of several alternative approaches for overcoming such difficulties

(Cannon, Percival, Caccia, Raymond, & Bassingthwaighte, 1997; Halley, 2009; Miramontes & Rohani, 2002; Pimm & Redfearn, 1988; Rohani, Miramontes, & Keeling, 2004).

Inaccuracies in estimation and differences across approaches can potentially filter through to generate statistical artefacts and important differences in population dynamics, affecting, for example, extinction risk forecasts (Halley & Kunin, 1999). Given the short time-scales typically available for ecological time-series data, two important questions in population biology are therefore: (a) what model form (e.g., white noise, autoregressive or 1/*f* process) best characterizes, and (b) what statistical power do we have for correctly detecting autocorrelation in the environmental variables that drive natural population fluctuations? Identifying the role of coloured environmental noise in driving population dynamics, moderating species interactions and shaping community structure is especially important in the context of climate change and the future challenges faced by biodiversity. Climate warming is expected to change the spatio-temporal structure of natural environmental fluctuations (Wigley, Smith, & Santer, 1998). For example, recent evidence suggests that El Niño years are increasing in frequency (Power, Delage, Chung, Kociuba, & Keay, 2013; i.e., becoming less red). In contrast, Northern Hemisphere weather systems are expected to start changing more slowly (i.e., becoming redder) because of amplified arctic warming causing weakened jet streams (Hurrel & Loon, 1997; Mann et al., 2017).

Previous efforts have been made to estimate the colour parameters of natural environmental variables (e.g., García-Carreras & Reuman, 2011; Vasseur & Yodzis, 2004). To date, however, no study has attempted to do this for multiple environmental variables that have been linked explicitly and robustly to natural animal population time series. Here, using abiotic environmental variables that have been appropriately coupled to population fluctuations across a wide range of terrestrial animal taxa and geographical locations (Knape & de Valpine, 2011), we have evaluated the statistical support for different colours and the underlying processes in the natural environmental variables associated with animal populations. This represents a useful step forward given (a) the lack of statistical support for many purported power-law relationships, such as those investigated here (Stumpf & Porter, 2012), and (b) the predicted sensitivity of population responses to the colour of environmental noise and the corresponding wide-ranging effects on species and their interactions with other species. Our initial aim was to investigate whether animal populations respond to a broad range of abiotic environmental drivers or to some subset of possible variables. We then assessed the level of statistical support and power in natural environmental time series for three models commonly used to characterize or simulate (coloured) stochastic processes: white noise (a purely random process without any temporal structure), AR(1) and 1/*f* models. Support for these methods was assessed by analysis in both the frequency and time domains (Chatfield, 1996; Dillon et al., 2016) to allow meaningful comparison across the methods. We also evaluated the multi-segmenting method (MSM) of Miramontes and Rohani (2002), especially designed for estimating 1/*f* colour coefficients from short time series. We recorded the frequency of different environmental coefficient estimates (including their confidence intervals) to (a) establish the evidence for different coloured environmental covariates associated with population fluctuations in different animal taxa, and (b) assess whether results are characterized by lack of statistical power using the relatively short (≤ 50-year) length of available animal population time series through comparison with longer (101-year) versions of the same associated environmental series.

2 | METHODS

2.1 | Data sources

We investigated abiotic environmental variables that were explicitly linked to natural population fluctuations as covariates in log-scale first- or second-order autoregressive models by Knape and de Valpine (2011). They carried out a large-scale analysis of natural population time series from the Global Population Dynamics Database (GPDD; NERC Centre for Population Biology, 1999), which were coupled with a range of geo-spatially matched environmental covariates and with indices for the North Atlantic Oscillation [Hurrel Station-Based DJFM (Winter) NAO Index] and Southern Oscillation (SO) annual Index. The coupling by Knape and de Valpine (2011) only used environmental covariates that significantly reduced the model process error variance when included in models fitted to the GPDD population time-series data. The spatially matched environmental variables were annual seasonal averages of monthly mean, maximum and minimum temperatures (calculated from the same temperature data) and of precipitation (in millimetres) and frost day frequency, obtained from the CRU TS v.2.1 database (Mitchell & Jones, 2005). These environmental variables provided the main data source for our present analysis, and details of how corresponding population and environmental time series were initially filtered are fully described by Knape and de Valpine (2011). We further filtered the available environmental series for analysis by selecting only those covariates that were selected in the most parsimonious model describing population fluctuations by Knape and de Valpine (2011) according to Akaike information criterion corrected for small sample size (AIC_C; 371 series out of 492) and had ≥ 10 consecutive (annual) data points. We excluded 10 further environmental time series that were not suitable for spectral analysis because they showed identical values for all except one data point. We also excluded 135 repeated series; if the same environmental variable was associated with the dynamics of several species, overlapping in time, only the part of the environmental variable with the longest corresponding population time series was used.

We performed the analyses both on the time interval for which population data were available in the matched GPDD natural population time series [following Knape & de Valpine (2011), hereafter referred to as the 'short' series] and on the entire series from the CRU TS v.2.1 database (years 1901–2002, the 'long' series). The latter approach increased statistical power under the assumption that

the same covariates also affected the corresponding populations before (or after) the populations had been surveyed. Given that winter series were composed of environmental data from December, January and February, the final year of the long series missed the last 2 months and was excluded. For consistency, we also removed the last year from the other environmental covariate types. Finally, 21 series were removed where no match between the original, short series and the long CRU series could be found. This left us with 163 unique short (≤ 50-year) and 160 unique long (101-year) environmental time series for our main analysis (Figure 1; Supporting Information Appendix S1 Table S1). All environmental time series were standardized to have zero mean and unit variance, and detrended (see 'Time series analysis and model comparison').

The terrestrial animal population time series were composed of annual abundance estimate data from birds, mammals and insects. We recorded the distributions of environmental covariate types and the classes of the associated animal series [in this analysis, all covariates related to temperature (mean, maximum and minimum seasonal averages) were pooled]. This left us with 224 unique animal population time series driven by the environment in our final analyses. For the long time series, we also recorded the proportions of animal classes associated with coloured or white environmental covariates (see 'Time series analysis and model comparison').

2.2 | Time series analysis and model comparison

We compared three statistical models commonly used to generate and/or characterize stochastic coloured time series: white noise, AR(1) and 1/*f* models. The white noise model (i.e., a random process with no temporal structure) is a special case of both latter models, but is described using one parameter less. To evaluate the strength of support for these models, we analysed data in the frequency domain, where we fitted the theoretical power spectra to the empirical periodograms of the detrended time series (detrending removed the least-squares straight-line fit with respect to year from the environmental time series, then used the residuals for further analysis). Given that detrending has the potential to 'whiten' power spectra, we also performed the main analysis using non-detrended data (see Supporting Information Appendix S2). This differs from the normal approach for AR(1) models, where parameters are generally estimated in the temporal domain. However, we first estimated the autocorrelation coefficients in the frequency domain to ensure that

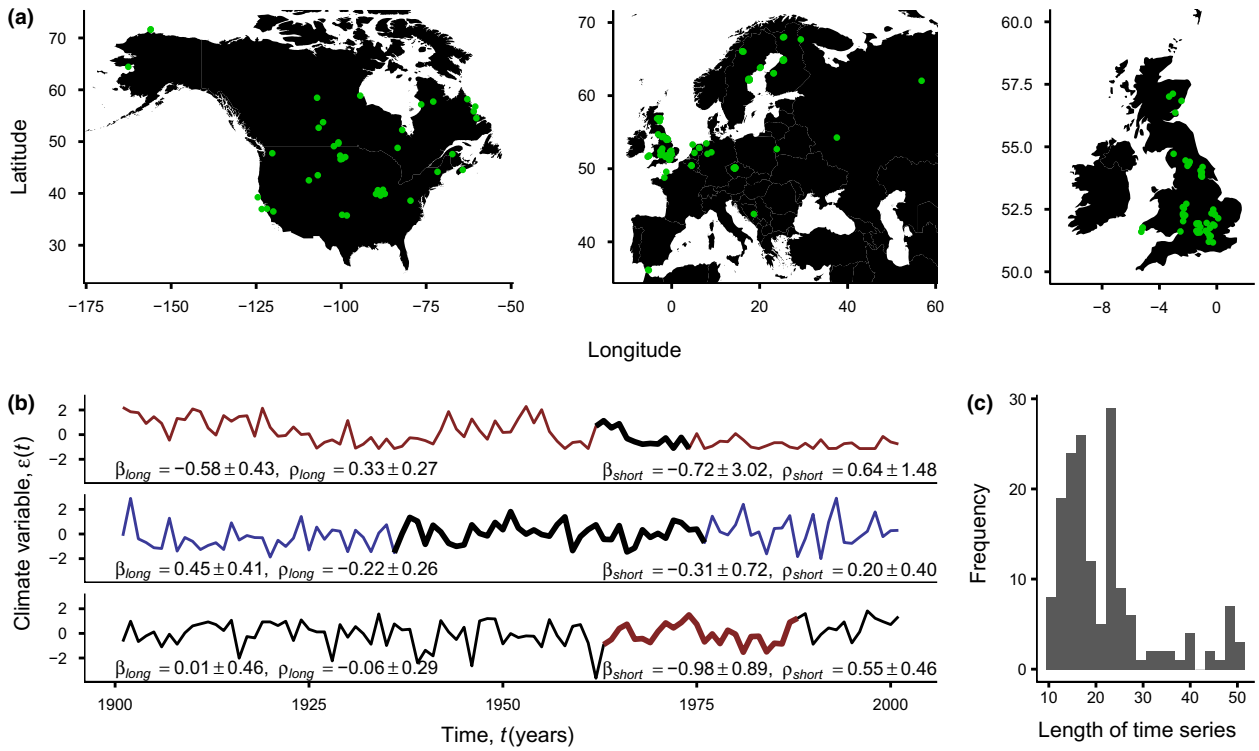

FIGURE 1 Characteristics of the environmental time series used in the study. (a) The geographical positions in U.S.A. and Canada (left), Eurasia (middle) and U.K. and Ireland (zoomed in, right) of the Global Population Dynamics Database (GPDD) natural population time-series data, whose fluctuations are associated with the geo-spatially linked environmental covariates analysed here (a small jitter is added to allow overlapping locations to be shown). (b) Three example environmental time series, coloured based on their associated colour parameters, estimated from the frequency domain (spectral exponent, β; autocorrelation coefficient, ρ_f (± 95% CIs); middle long series is defined as 'blue' based on β alone; black series denote white noise). Upper, middle and lower environmental series show summer frost day frequency, summer precipitation and winter minimum temperature, associated with population dynamics of *Euphydryas editha* (bay checkerspot butterfly), *Contopus virens* (eastern wood-pewee) and *Libellula quadrimaculata* (four-spotted chaser), respectively (thick part of lines shows dates corresponding to available animal population data). (c) Length (in years) of the short time series used in the analyses; median = 18 years

the competing models compared the same data. The empirical periodograms (power spectra) were obtained with a standard fast Fourier transform algorithm using the 'fft' function in MATLAB (v.2014a), where the number of frequencies evaluated equals $ceil\left[(n+1)/2\right]-1$ (*ceil* rounds a number to the next larger integer).

The theoretical power spectrum of the AR(1) model is (Chatfield, 1996, p. 100):

$$P(f)=\frac{\sigma^2}{1+\rho^2-2\rho\cos(2\pi f)} \quad (1)$$

where ρ is the autocorrelation parameter and σ is the standard deviation of the (environmental) time series. For $1/f$ (short for $1/f^{\beta}$) processes, the corresponding function is:

$$P(f)=10^{\alpha+\beta\log_{10}f} \quad (2)$$

where β is the spectral exponent (slope) and α is a constant regulating the intercept of the spectrum and thus the strength of fluctuations.

The theoretical power spectral densities were fitted to the periodograms on the decibel scale (any logarithmic scale would be valid and will not affect our conclusions), using a least-squares approach. The decibel transformation is a special case of logarithmic transformation, namely:

$$dB(x)=10\log_{10}x \quad (3)$$

That is, the power was decibel transformed (the *dB* operator is scaled logarithmically) before model fitting, making the multiplicative model additive.

To evaluate the white noise model, we fitted a linear regression with an intercept only:

$$dB\left[P(f_i)\right]=\alpha_1+\varepsilon_f \quad (4)$$

where f_i is the empirical periodogram and ε_f are normal, independent, identically distributed residuals.

For the AR(1) process, we fitted the model:

$$dB\left[P(f_i)\right]=\alpha_2-dB\left[1+\rho^2-2\rho\cos(2\pi f)\right]+\varepsilon_f \quad (5)$$

solving for the maximum likelihood (i.e., least-squares) solution for parameter ρ, using the function 'fminbnd' in MATLAB (v.2014a) for one-dimensional nonlinear minimization. We used ordinary least squares to fit the remaining parameters in each iteration. The intercept α_2 then corresponds to $dB(\sigma^2)$ (see Equation 1).

The power spectrum for the $1/f$ process is linear on the log–log scale and can be fitted as:

$$dB\left[P(f_i)\right]=\alpha_3+\beta\, dB(f)+\varepsilon_f \quad (6)$$

where the intercept α_3 corresponds to 10α (see Equation 2).

We recorded parameter estimates from the frequency domain for the spectral exponent (β) and autocorrelation coefficient (ρ_f) for each time series, and symmetric 95% confidence intervals (CIs) for each estimate, based on the *t*-distribution. The statistical significance of parameter estimates was determined by assessing whether the range of the 95% CIs of the estimate spanned zero. Furthermore, we estimated the autocorrelation coefficient (± 95% CIs) from the temporal (time) domain (ρ_T), in common with the majority of previous work. This allowed us to determine whether the loss of power associated with estimating autocorrelation in the frequency domain (where *ca. n*/2 data points are used in the coefficient estimation) had an important influence on our results and conclusions. We also compared colour coefficients with a null hypothesis of intermediately reddened colour, generally referred to as pink noise in the frequency domain (e.g., Halley, 1996), here considered to represent ecologically non-trivial temporal structure on the annual scale. Given that the true underlying process for environmental fluctuations is unknown, this was done by checking whether CIs of the estimates spanned $\beta = -1$ for the $1/f$ models and $\rho_f = \rho_T = 0.7$ for the AR(1) models. We note that $1/f$ noise has no characteristic time-scales, and a pink noise spectrum contains equal density influences (memory) on all time-scale intervals if expressed on an octave scale (Halley, 1996; Halley & Kunin, 1999; Keshner, 1982), whereas the characteristic time-scale, τ, of a AR(1) process is defined by $\rho = \exp(-1/\tau)$ (i.e., for $\rho = 0.7$, $\tau = 2.804$ years). However, for simplicity, we refer here to $\beta = -1$ and $\rho_f = \rho_T = 0.7$ as pink noise.

To compare relative model performance in the frequency domain, we recorded AIC_C values from the $1/f$, AR(1) and white noise models. Using AIC_C values, we calculated model weights (w_i) and evidence ratios (E_i) as follows:

$$w_i=\frac{\exp\left(-\frac{1}{2}\Delta AIC_{Ci}\right)}{\sum_{r=1}^{R}\exp\left(-\frac{1}{2}\Delta AIC_{Cr}\right)} \quad (7)$$

and

$$E_{\min,i}=\frac{w_{\min}}{w_i}=\exp\left(-\frac{1}{2}\Delta AIC_{Ci}\right) \quad (8)$$

where $\Delta AIC_{Ci} = AIC_{Ci} - AIC_{Cmin}$, and R is the total number of models being compared (Anderson, 2008).

Finally, given that the detection of colour in short time series is difficult, we also evaluated the MSM of Miramontes and Rohani (2002), suggested to improve accuracy of $1/f$ colour estimates from time series as short as 47 time points (see Supporting Information Appendix S3).

2.3 | Power analysis for colour estimates

The power for detecting trends in, for example, time-series data, using least-squares linear regression, can be derived from the relationship between the slope, *b* (corresponding here to either ρ or β), the number of data points, *n*, the variance of the residuals, σ^2_{res}, and of the independent variable, σ^2_x, of the regression (Gerrodette, 1987):

$$b^2 n\sigma_x^2 \geq (z_{A/2}+z_B)^2\sigma_{res}^2 \quad (9)$$

where z_A (z_B) is the value of a standard normal variable where the area under one tail of the probability density function beyond z_A (z_B) is A (B). That is, A is the probability of having a type I error (rejecting the null-hypothesis, H_0, even if no true trend exists) and B is the probability of having a type II error (not rejecting H_0 even if a true trend exists). Power (1 – B) is then the probability of avoiding type II errors (correctly rejecting H_0).

Using Equation 9 and the normal cumulative density function, Φ, power (1 – B) can be calculated as a function of b, n, σ_x^2, σ_{res}^2 and $z_{A/2}$ (A):

$$power = 1-\Phi\left(z_{A/2}-\sqrt{\frac{b^2 n\sigma_x^2}{\sigma_{res}^2}}\right) \quad (10)$$

To evaluate our power to conclude correctly that colour coefficients (b in Equations 9 and 10) from regressions failing to reject our null hypothesis are not significantly different from zero, we performed a retrospective power sensitivity analysis (Gerrodette, 1987; Peterman, 1990; Thomas, 1997), varying b from zero to two in increments of 0.01. By rearranging Equation 9 we also evaluated the smallest detectable colour and the time-series length needed to recognize a specific colour, for a given level of power. The analyses were performed using the observed residual and independent variable variances from the linear least-squares regressions in the frequency ($1/f$; Equation 6) and time domains, using data from the short and long environmental time series, with A = 0.05.

Our power analysis is based on standard least-squares linear regression (Gerrodette, 1987). Estimates for AR models have a different sampling distribution, and the power formulas (Equations 9 and 10) are not strictly correct when $|\rho_T|$ approaches one and the AR(1) process is no longer stationary. We therefore performed a simulation-based power analysis using long artificial time series of known colour to confirm our results. Given that the AR(1) process in the frequency domain (Equation 5) is nonlinear, this was not included at all in the power analysis.

3 | RESULTS

3.1 | Environmental variable types and species responses

Among the environmental variables analysed, those related to temperature were associated with the fluctuations of the largest fraction (42%) of populations, whereas the NAO (5%) and SO (8%) climate indices affected the smallest fractions of populations (Figure 2a). Precipitation and frost day frequency influenced the fluctuations of 23 and 21% of the population time series, respectively. Seasonally, environmental covariates related to spring were associated with the largest fraction (30%) of all variables, with the remaining 25% summer, 24% winter and 20% autumn variables (Figure 2a). In total, 224 unique terrestrial animal populations were associated with 163 environmental covariates, where 126 (56%) were bird populations, 69 (31%) insects and 29 (13%) were mammals, respectively (Figure 2b). Given the potential for taxonomic selection bias (over-representation of some species/taxa) present in the original GPDD database, we did not compare our results with the underlying percentages from the GPDD or CRU data sets.

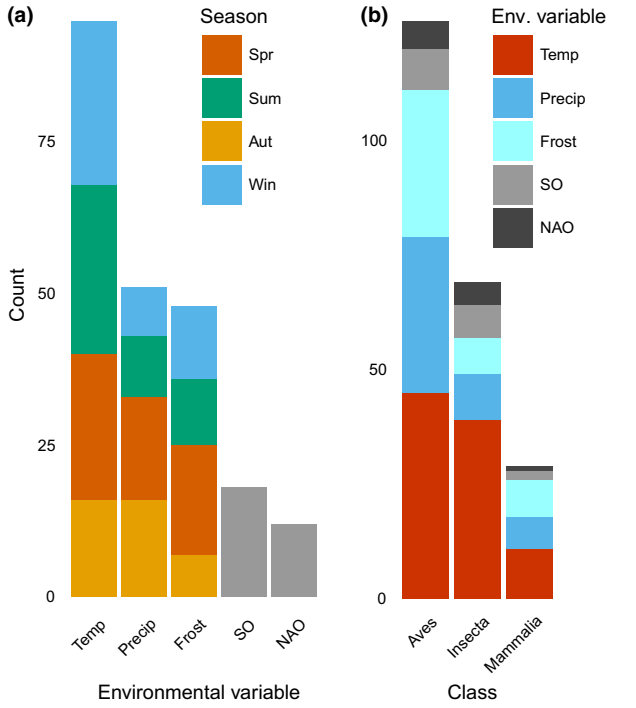

FIGURE 2 (a, b) The distribution of (a) environmental variable types, associated with (b) fluctuations in different terrestrial animal population taxa. All environmental variables related to temperature [Temp (mean, maximum and minimum seasonal averages)] were pooled because they were based on the same temperature data (Mitchell & Jones, 2005). Precip and Frost denote precipitation and frost day frequency, respectively. There were n = 224 unique population time series associated with both (a) and (b). There were 163 unique environmental variable time series in (a), because the El Niño Southern Oscillation (SO) and North Atlantic Oscillation (NAO) indices are associated with several populations

3.2 | Temporal analysis of environmental time series

Out of 163 environmental series (S, ≤ 50 years), most were indistinguishable from white noise processes (Figure 3). Analysis of the entire, longer environmental series (L, 101 years) showed a larger fraction of estimates being significantly different from zero (Figure 3d–f) compared with short series (Figure 3a–c); the estimates that were distinguishable from white noise processes tended to be reddened (Figure 3d–f). The means of the estimated colour coefficients (± 95% CIs) were $\mu(\beta_S)$ = −0.088 ± 0.116; $\mu(\beta_L)$ = −0.086 ± 0.038; $\mu(\rho_{fS})$ =

0.053 ± 0.052; $\mu(\rho_{fL})$ = 0.047 ± 0.023; $\mu(\rho_{TS})$ = 0.028 ± 0.036 and $\mu(\rho_{TL})$ = 0.102 ± 0.020.

Specifically, when colour exponents were estimated in the frequency domain, a white noise model was considered the best and most parsimonious fit to the short data series in 151 (93%) cases, while 1/*f* and AR(1) models were considered best in seven (4%) and five (3%) of cases, respectively (Figures 3 and 4). Only two (1%) of the parameter estimates were found to differ significantly from zero under both 1/*f* and AR(1) models. These general patterns are reflected in the longer time series; 106 (66%) were best described by

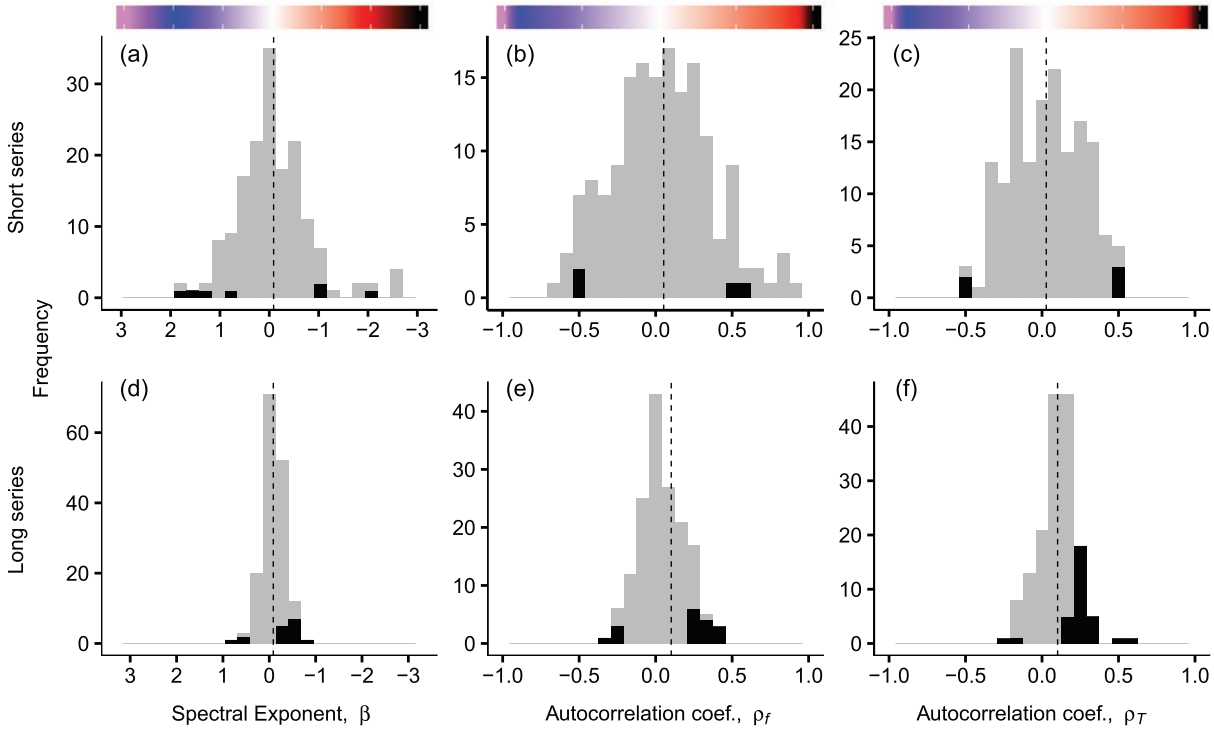

FIGURE 3 Estimated colour coefficients from environmental variables associated with natural, terrestrial animal population fluctuations. Grey bars show the frequency of point estimates for different colours; black bars show only those estimates that were significantly different from zero. (a, d) Spectral exponents (β). (b, e) Autocorrelation coefficients (ρ_f) estimated from the frequency domain. (c, f) Autocorrelation coefficients estimated from the time domain (ρ_T). Panel rows show results based on short (a–c; *n* = 163) and long (d–f; *n* = 160) time series. Bars above the top row indicate the corresponding colour of the estimated coefficients. Vertical dashed lines show mean values across all estimated coefficients

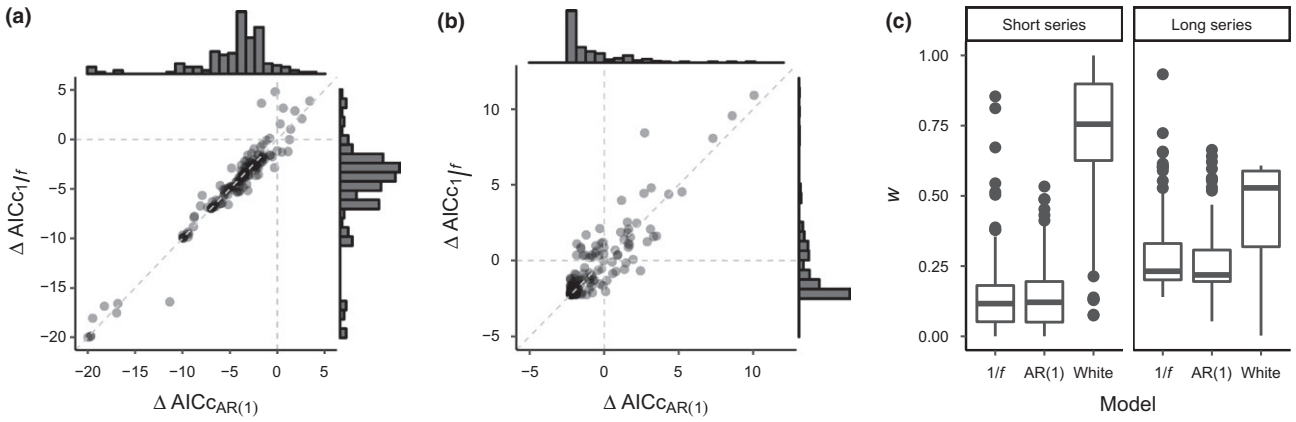

FIGURE 4 Comparison of the relative performance of three modelling approaches describing temporal environmental variation evaluated in the frequency domain. (a, b) Differences in Akaike information criterion corrected for small sample size (AIC_C) values for white noise, 1/*f* and AR(1) models. The $\Delta AIC_{C\ AR(1)}$ and $\Delta AIC_{C\ 1/f}$ show the difference between white noise and AR(1), and white noise and 1/*f* models, respectively. Negative values indicate white noise being the best (more parsimonious) model. Points are semi-transparent to visualize overlaps. Panels present results based on (a) short and (b) long environmental series. (c) The AIC_C weights (*w*) for models based on short (left) and long (right) time series

white noise, 33 (21%) by 1/*f* and 21 (13%) by AR(1) models (Figures 3 and 4), with 11 (7%) of the longer time series differing significantly from zero under both 1/*f* and AR(1) models. Of these, the majority (10) were reddened, and only one was blue. We also performed this analysis without detrending the weather data, to ensure our analyses of colour coefficients were not biased by our method of detrending the time series. We found a weak whitening effect attributable to our detrending approach in our main analysis (Supporting Information Appendix S2, Figure S2.1), more so in the short series compared with the long series. The means of the estimated colour coefficients (± 95% CIs) using the un-detrended (raw) data were $\mu(\beta_S) = -0.240 \pm 0.111$; $\mu(\beta_L) = -0.165 \pm 0.038$; $\mu(\rho_{f\,S}) = 0.118 \pm 0.053$ and $\mu(\rho_{f\,L}) = 0.083 \pm 0.024$. Comparing colour exponents from the main analysis in the frequency domain with estimates from the MSM did show slightly stronger colours using the MSM on the short series, but not for the long series. The means of the estimated colour coefficients (± 95% CIs) using the MSM method were $\mu(\beta_S) = -0.243 \pm 0.129$ and $\mu(\beta_L) = -0.114 \pm 0.034$ (Supporting Information Appendix S3).

Considering relative model performances from the frequency domain, the mean difference (± 95% CIs) between AIC_C values from white noise and 1/*f* or AR(1) models for the short time series were similar: $\mu(\Delta AIC_C[1/f_S]) = -4.544 \pm 0.635$ and $\mu(\Delta AIC_C[AR(1)_S]) = -4.533 \pm 0.620$ (Figure 4a). There was a greater difference in model performance for the long time series, although variation around the mean differences remained high: $\mu(\Delta AIC_C[1/f_L]) = -0.634 \pm 0.353$ and $\mu(\Delta AIC_C[AR(1)_L]) = -0.785 \pm 0.325$ (Figure 4b). When comparing 1/*f* and AR(1) models, the ΔAIC_C values were −0.011 ± 0.160 (short series) and −0.151 ± 0.161 (long series), and AIC_C weights (normalized model relative likelihoods) showed comparable support for both models (Figure 4c; Supporting Information Appendix S1, Figure S1.1). The AIC_C weights consistently supported white noise models in the shorter time series, with an increase in relative likelihood for both 1/*f* and AR(1) models describing the longer time series (Figure 4c; Supporting Information Appendix S1, Figure S1.1).

Colour coefficients can also be compared with a 'null' hypothesis of pink noise ($\beta = -1$, $\rho_f = 0.7$). Spectral exponent (β) 95% CIs included pink noise in 98 (60%) of short time series and only two (1%) estimated from long time series. Autocorrelation coefficient (ρ_f) CIs included pink noise in 70 (43%) short series and two (1%) of the long series.

Five (3%) of the 163 autocorrelation coefficients estimated in the temporal domain (ρ_T) from short time series were found to differ significantly from zero (Figure 3c). For the 160 long series, 32 (20%) of the estimates differed significantly from zero (Figure 3f). The mean ρ_T estimates were $\mu(\rho_{T\,S}) = 0.028 \pm 0.036$ and $\mu(\rho_{T\,L}) = 0.102 \pm 0.020$ (Figure 3c, f), with strong correlations between the colour coefficient estimates from 1/*f* and AR(1) methods (Supporting Information Appendix S1, Figure S1.2).

We found that larger fractions of the coloured environmental covariates were associated with mammals, whereas smaller fractions were associated with birds, compared with the white covariates (Supporting Information Appendix S1, Figure S1.3). Averaged over all models, 20 (14%) and seven (32%) cases of the long environmental time series characterized as white or coloured, respectively, were associated with population time series of mammals, 88 (64%) and 10 (46%) cases, respectively, with birds, and 30 (22%) and five (22%) cases, respectively, with insects (Supporting Information Appendix S1, Figure S1.3). Given that sample sizes for coloured fractions were very low (Supporting Information Appendix S1, Figure S1.3), we did not test for significant differences between fractions.

3.3 | Power analysis for colour estimates

The statistical power to identify a coloured signal from white noise correctly was, as expected, higher for the long time series compared with the short, and in the time domain compared with the frequency domain (Figure 5a). Mean power values (± 95% CIs) for pink environments ($|\beta| = 1$, $\rho_T = 0.7$) were 0.575 ± 0.041 and 0.865 ± 0.016 (short series), and 0.995 ± 0.002 and 1.000 ± 0.000 (long series), respectively. Consequently, the smallest detectable colour is lowest in the time domain using the long time series and highest in the frequency domain using the short series (Figure 5b). Moreover, the time-series length required to detect colour correctly increases rapidly for colour close to white noise (Supporting Information Appendix S1, Figure S1.4). Correct detection of, for example, pink noise with power 0.8 would require at least 47 ± 6 data points in the frequency domain ($\beta = 1$) or 16 ± 1 points in the time domain ($\rho_T = 0.7$) based on the short series, whereas correct identification of a signal with a colour exponent $|\beta| = 0.1$ with power 0.8 would require at least 4,637 ± 583 points in the frequency domain.

4 | DISCUSSION

We have shown that the majority (93%) of environmental variables that have previously been linked to terrestrial animal population fluctuations do not appear to show any recognizable temporal structure (colour), when estimated over a maximum of 50 years. However, there is considerable uncertainty associated with the colour estimates for these short series, indicated by wide confidence intervals (Supporting Information Appendix S1, Table S1). Our power analysis (Figure 5) clarifies this uncertainty; power is not high enough to draw strong conclusions in the frequency domain using the short series; however, in the time domain, we can be relatively certain (power *ca*. 0.8) that we correctly identified any pink noise ($\rho_T \geq 0.7$) in environmental series of ≥ 16 years, corresponding to 69% of our short time series. When longer (101-year) versions of the matched environmental time series were used, 34% were best described by a coloured noise, either 1/*f* or AR(1), process in the frequency domain, and the estimates that were distinguishable from white noise processes tended to be reddened. In the time domain, 32 of the 160 (20%) long series were distinguishable from white noise. Here, power is sufficiently high (0.95) for us to be confident that any pink (or blue) noise in the frequency domain ($|\beta| \geq 1$) and coloured noise with an absolute estimate $|\rho_T| \geq 0.35$ in the time domain were correctly detected. If a

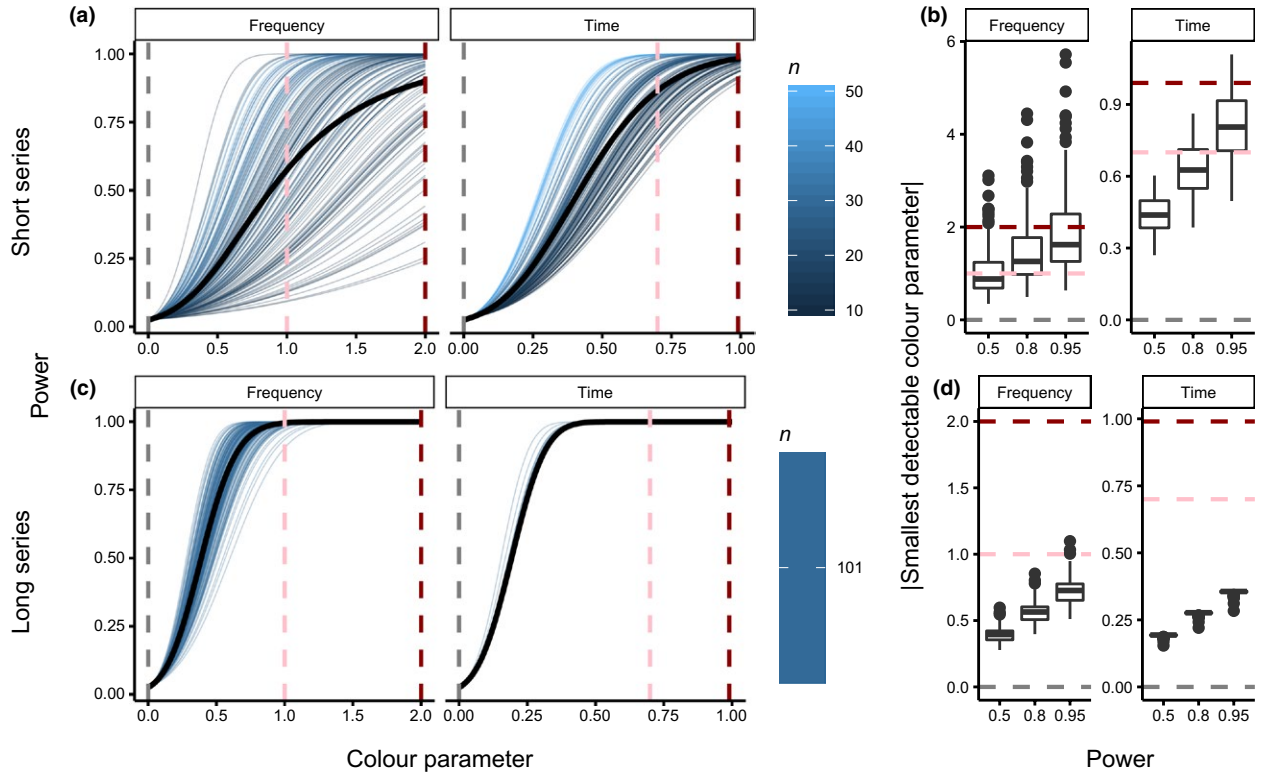

FIGURE 5 Power functions (a, c) and absolute values of smallest detectable colour parameter (b, d) for 1/*f* models in the frequency and AR(1) models in the time domains, for short (*n* = 10–50 years; a, b) and long (*n* = 101 years; c, d) environmental variables associated with natural, terrestrial animal population fluctuations. Thick lines in (a, c) are the mean for all series. Dashed lines show white ($\beta = \rho_T = 0$), pink/blue ($|\beta| = 1$, $|\rho_T| = 0.7$) and red/violet ($|\beta| = 2$, $|\rho_T| = 0.99$) noise in the two domains. A power of, for example, 0.8 equals the risk of a type II error of 0.2 (four times higher than a type I error risk of 0.05). Note the varying scales in (b, d)

power of 0.8 is considered, we correctly identified coloured noise with an estimate $|\rho_T| \geq 0.27$. Only 2% of the covariates (7% for the long series) were consistently considered coloured under both 1/*f* and AR(1) models. Temperature was the most common environmental variable associated with the animal population fluctuations (42%), although precipitation and frost day frequency were both associated with sizeable proportions of the populations (23 and 21%, respectively; Figure 2). Comparing the fractions of coloured or white environmental covariates associated with animal classes, mammals and birds showed the largest differences; 14, 64 and 22% of the long environmental time series characterized as white were associated with mammals, birds and insects, respectively, whereas the corresponding percentages characterized as coloured were 32, 46 and 22%.

Although there were fewer white noise series among the longer (101-year) environmental time series examined, extrapolated beyond the range of available population data, the model forms selected and colour coefficients estimated generally agreed with the results from the short series. However, the colour of environmental variables is known to be dependent on the time-scale considered (e.g., Halley, 2007; Kirchner, 2005; Miramontes & Rohani, 2002; Pimm & Redfearn, 1988; Sabo & Post, 2008). The level of support for coloured time series should increase with the length of the series, because fluctuations at low (compared with high) frequencies require a longer time to be detected. Indeed, the entire distribution of model evidence ratios was slightly shifted in the direction of support for coloured processes, comparing the long series with the short (Supporting Information Appendix S1, Figure S1.1). Including the longer environmental series improves our statistical power for detecting colour (Figure 5; Supporting Information Appendix S1, Figure S1.4) at the cost of weakening the empirical link to population dynamics, because the coupled animal population time series were not as long. Examining the environmental time series in the temporal domain also increases statistical power, mainly owing to loss of data in the frequency domain where the number of degrees of freedom is around half of that compared with the time domain. Clearly, the time domain offers an advantage when it comes to identifying correctly colour coefficients close to white noise in the sorts of data sets typically available to ecologists. The lack of longer (> 101-year) environmental time series could also be why we found such small differences between the 1/*f* and the AR models (Halley, 2005), and the reason why the MSM approach showed the same results as the main analysis (Supporting Information Appendix S3). Our short and long series provided only up to three or four segment sizes, respectively, for the MSM regression (Supporting Information Appendix S3, Figure S3.1).

Our analysis was based on covariates linked to population fluctuations where changes in population sizes were recorded annually; any cycles with a period shorter than 1 year are therefore not present in the data. Organisms with shorter life spans, for example, having multiple generations within a single year, might therefore show different results. In the case of red environmental noise, extinction risk decreases in annually reproducing species, but increases for semelparous and perennial species (Heino & Sabadell, 2003). The long environmental time series analysed here ran from 1901 to 2002, and as longer time series (with a higher temporal resolution) become available, we recommend re-analysis based on the approach used here.

Power law relationships are often proposed to describe natural patterns, although few of them are backed up statistically (Stumpf & Porter, 2012). Our results illustrate that there is little support for power law characteristics in the temporal structure [i.e., heavy tailed distributions of slow or rapid fluctuations (low or high frequencies)] of most of the environmental covariates analysed here. That is, we found weak support for recognizable temporal structure (colour) with an absolute colour coefficient in the time domain ≥ 0.27 in annual variables associated with terrestrial animal population fluctuations. Previous work has suggested that the colour of a number of terrestrial environmental variables is distributed between white and pink noise (Vasseur & Yodzis, 2004). Our approach builds on this earlier analysis by incorporating further statistical context to improve our understanding. García-Carreras and Reuman (2011) suggested that there was a correlation between animal population and environmental spectral exponents, also using data from the GPDD. However, a correlation analysis between the colour parameter of an environmental signal and that of raw population sizes ignores density-dependent feedback mechanisms and uncertainty in parameter estimates, and can easily generate spurious correlations (Royama, 1981). We avoided those problems here using only the environmental covariates identified as meaningful components in population models by Knape and de Valpine (2011). Although part of this coupling identified may be weak owing to possible model overfitting (Knape & de Valpine, 2011), it is the only study we are aware of in which a robust statistical model selection framework has been used to link empirical population time-series fluctuations with environmental covariates [but see Ferguson, Carvalho, Murillo-García, Taper, & Ponciano (2016) for a simulation study].

Given that relatively few environmental variables associated with population dynamics are temporally autocorrelated, this should be put into context with a few recent studies providing indirect support to our results. Using a model-based approach, Ferguson et al. (2016) estimated the degree of environmental autocorrelation present in time series of animal population data and, as in the present study, found it to be low. Engen et al. (2013) developed a theoretical method using age-structured populations for estimating the influence of autocorrelated environments on population dynamics. When applied to data sets from four mammal species, they found small effects of autocorrelated environments on population dynamics and concluded that using white noise approximations is often appropriate. This is also argued by van de Pol et al. (2011), who found that the extinction risk of a shorebird population was largely insensitive to noise colour because of the poor tracking ability of demographic rates on the colour of the environment. None of the three studies above analysed the temporal structure of environmental variables per se. However, taken together, it is clear that a new perspective on the role of coloured environments is starting to emerge. Given that many ecological factors, such as species extinction risk and ecosystem function and stability, depend on the colour of the environment that populations are exposed to (e.g., Gudmundson et al., 2015; Ripa & Ives, 2003; Ruokolainen, Lindén, et al., 2009), incorporating empirically supported noise processes into predictive models of population and community dynamics is crucial for their reliability. Furthermore, when non-white colours have been detected reliably in environmental series, we can ask whether this coloured noise is ecologically relevant. This will depend on, for example, the demographic details of the population being affected, such as the intrinsic growth rate and shape of density dependence (Ruokolainen, Ranta, et al., 2009; Fowler & Ruokolainen, 2013b), but it is largely still an open question of considerable ecological interest.

Our results have implications for understanding the temporal structure of environmental variation driving terrestrial animal population dynamics. Temperature was shown to be the most important weather variable associated with population dynamics, but our data sets were confined to the Northern Hemisphere with strong seasonal effects, as also evidenced by the important role of frost days. Environmental time series from a wider range of geographical locations might reveal that other variables also have an important impact. Our main analysis did not include long-term environmental change (owing to our detrending approach) or its impact on species in marine environments. In contrast to the terrestrial environment, marine environmental change is largely red because of the inertia in large bodies of water to rapid and/or dramatic fluctuations (Steele, 1985; Vasseur & Yodzis, 2004). For both environments, however, there is increasing concern about how climate change will alter the colour of environmental noise and the corresponding impact this will have on the dynamics of species. Recent evidence suggests that the colour of some weather variables is becoming both more blue (e.g., El Niño years increasing in frequency; Power et al., 2013) and red (e.g., Northern Hemisphere weather systems start changing more slowly; Hurrel & Loon, 1997; Mann et al., 2017). Such changes could have profound implications for biodiversity across the globe.

Based on the results presented here, we propose that for time spans typical for ecological time series, white noise or weakly reddened processes often best describe the annually measured abiotic environmental variables that are associated with fluctuations in many terrestrial animal populations, and analyses of coloured processes are best performed in the time domain to maximize confidence in parameter estimates. Given that population trajectories themselves are often autocorrelated, this implies that intrinsic and extrinsic biotic factors such as density dependence, age structure and species interactions are the most likely cause for such fluctuations (see

e.g., Akçakaya, Halley, & Inchausti, 2003; Ferguson et al., 2016). However, more effort is needed to collect coupled population and environmental data over longer time spans to ensure that the importance of coloured environmental processes is not underestimated.

5 | ACKNOWLEDGMENTS

D.G., M.S.F., M.M. and S.M.S. were supported by the Natural Environment Research Council (NERC) grants NE/N002849/1 and NE/N00213X/1.

AUTHOR CONTRIBUTIONS

M.S.F. developed the original idea, further developed by D.G.; D.G., M.S.F. and A.L. contributed to data analysis, and all authors contributed to data interpretation and manuscript preparation, led by D.G.

DATA ACCESSIBILITY

All high-resolution gridded climate covariates analysed in this study are available from the University of East Anglia Climatic Research Unit (CRU): https://crudata.uea.ac.uk/cru/data/hrg/

The North Atlantic Oscillation [Hurrel Station-Based DJFM (Winter) NAO] Index is available from the University Corporation for Atmospheric Research and National Center for Atmospheric Research Climate Data Guide: https://climatedataguide.ucar.edu/climate-data/hurrell-north-atlantic-oscillation-nao-index-station-based

The Southern Oscillation annual Index (SOI) is available from the Australian Government Bureau of Meteorology: https://www.bom.gov.au/climate/current/soihtm1.shtml

The GPDD population data are available from the Centre for Population Biology, Imperial College London: https://www.imperial.ac.uk/cpb/gpdd2/

ORCID

David Gilljam http://orcid.org/0000-0001-7421-945X

REFERENCES

Akçakaya, H. R., Halley, J. M., & Inchausti, P. (2003). Population-level mechanisms for reddened spectra in ecological time series. *Journal of Animal Ecology*, *72*, 698–702. https://doi.org/10.1046/j.1365-2656.2003.00738.x

Anderson, D. R. (2008). *Model Based Inference in the Life Sciences: A Primer on Evidence*. New York: Springer-Verlag.

Cannon, M. J., Percival, D. B., Caccia, D. C., Raymond, G. M., & Bassingthwaighte, J. B. (1997). Evaluating scaled windowed variance methods for estimating the Hurst coefficient of time series. *Physica A: Statistical Mechanics and its Applications*, *241*, 606–626. https://doi.org/10.1016/S0378-4371(97)00252-5

Chatfield, C. (1996). *The analysis of time series: An introduction* (5th ed.). London, New York, Washington DC: Chapman & Hall/CRC.

Coulson, T., Catchpole, E. A., Albon, S. D., Morgan, B. J. T., Pemberton, J. M., Clutton-Brock, T. H., … Grenfell, B. T. (2001). Age, sex, density, winter weather, and population crashes in soay sheep. *Science*, *292*, 1528–1531. https://doi.org/10.1126/science.292.5521.1528

Cuddington, K. M., & Yodzis, P. (1999). Black noise and population persistence. *Proceedings of the Royal Society B: Biological Sciences*, *266*, 969–973.

Dillon, M. E., Woods, H. A., Wang, G., Fey, S. B., Vasseur, D. A., Telemeco, R. S., … Pincebourde, S. (2016). Life in the frequency domain: The biological impacts of changes in climate variability at multiple time scales. *Integrative and Comparative Biology*, *56*, 14–30. https://doi.org/10.1093/icb/icw024

Engen, S., Sæther, B.-E., Armitage, K. B., Blumstein, D. T., Clutton-Brock, T. H., Dobson, F. S., … Ozgul, A. (2013). Estimating the effect of temporally autocorrelated environments on the demography of density-independent age-structured populations. *Methods in Ecology and Evolution*, *4*, 573–584. https://doi.org/10.1111/2041-210X.12043

Ferguson, J. M., Carvalho, F., Murillo-García, O., Taper, M. L., & Ponciano, J. M. (2016). An updated perspective on the role of environmental autocorrelation in animal populations. *Theoretical Ecology*, *9*, 129–148. https://doi.org/10.1007/s12080-015-0276-6

Fowler, M. S., & Ruokolainen, L. (2013a). Colonization, covariance and colour: Environmental and ecological drivers of diversity–stability relationships. *Journal of Theoretical Biology*, *324*, 32–41.

Fowler, M. S., & Ruokolainen, L. (2013b). Confounding environmental colour and distribution shape leads to underestimation of population extinction risk. *PLoS One*, *8*, e55855.

García-Carreras, B., & Reuman, D. C. (2011). An empirical link between the spectral colour of climate and the spectral colour of field populations in the context of climate change. *Journal of Animal Ecology*, *80*, 1042–1048. https://doi.org/10.1111/j.1365-2656.2011.01833.x

Gerrodette, T. (1987). A power analysis for detecting trends. *Ecology*, *68*, 1364–1372. https://doi.org/10.2307/1939220

Gonzalez, A., & Feo, O. D. (2007). Environmental variability modulates the insurance effects of diversity in non-equilibrium communities. In D. A. Vasseur & K. S. McCann (Eds.), *The impact of environmental variability on ecological systems. The Peter Yodzis fundamental ecology series* (pp. 159–177). Dordrecht, the Netherlands: Springer.

Greenman, J. V., & Benton, T. G. (2005). The impact of environmental fluctuations on structured discrete time population models: Resonance, synchrony and threshold behaviour. *Theoretical Population Biology*, *68*, 217–235. https://doi.org/10.1016/j.tpb.2005.06.007

Gudmundson, S., Eklöf, A., & Wennergren, U. (2015). Environmental variability uncovers disruptive effects of species' interactions on population dynamics. *Proceedings of the Royal Society B: Biological Sciences*, *282*, 20151126.

Hallett, T. B., Coulson, T., Pilkington, J. G., Clutton-Brock, T. H., Pemberton, J. M., & Grenfell, B. T. (2004). Why large-scale climate indices seem to predict ecological processes better than local weather. *Nature*, *430*, 71–75. https://doi.org/10.1038/nature02708

Halley, J. M. (1996). Ecology, evolution and 1/*f*-noise. *Trends in Ecology and Evolution*, *11*, 33–37. https://doi.org/10.1016/0169-5347(96)81067-6

Halley, J. M. (2005). Comparing aquatic and terrestrial variability: At what scale do ecologists communicate? Bridging the gap between aquatic and terrestrial ecology. *Marine Ecology. Progress Series*, *304*, 274–280.

Halley, J. M. (2007). *How do scale and sampling resolution affect perceived ecological variability and redness?* In D. A. Vasseur & K. S. McCann (Eds.), *The impact of environmental variability on ecological systems. The Peter Yodzis fundamental ecology series* (pp. 17–40). Dordrecht, the Netherlands: Springer.

Halley, J. M. (2009). Using models with long-term persistence to interpret the rapid increase of Earth's temperature. *Physica A: Statistical Mechanics and its Applications*, *388*, 2492–2502. https://doi.org/10.1016/j.physa.2009.02.027

Halley, J. M., & Kunin, W. E. (1999). Extinction risk and the 1/*f* family of noise models. *Theoretical Population Biology*, *56*, 215–230. https://doi.org/10.1006/tpbi.1999.1424

Heino, M., & Sabadell, M. (2003). Influence of coloured noise on the extinction risk in structured population models. *Biological Conservation*, *110*, 315–325. https://doi.org/10.1016/S0006-3207(02)00235-5

Hurrell, J. W., & Loon, H. V. (1997). Decadal variations in climate associated with the north Atlantic oscillation. *Climatic Change*, *36*, 301–326.

Hurst, H. (1951). Long-term storage capacity of reservoirs. *Transactions of the American Society of Civil Engineers*, *116*, 770–808.

Inchausti, P., & Halley, J. (2003). On the relation between temporal variability and persistence time in animal populations. *Journal of Animal Ecology*, *72*, 899–908. https://doi.org/10.1046/j.1365-2656.2003.00767.x

Keshner, M. S. (1982). 1/f noise. *Proceedings of the IEEE*, *70*, 212–218. https://doi.org/10.1109/PROC.1982.12282

Király, A., & Jánosi, I. M. (2002). Stochastic modeling of daily temperature fluctuations. *Physical Review E*, *65*, 051102. https://doi.org/10.1103/PhysRevE.65.051102

Kirchner, J. W. (2005). Aliasing in 1/f noise spectra: Origins, consequences, and remedies. *Physical Review E*, *71*, 066110.

Knape, J., & de Valpine, P. (2011). Effects of weather and climate on the dynamics of animal population time series. *Proceedings of the Royal Society of London B: Biological Sciences*, *278*, 985–992.

Lögdberg, F., & Wennergren, U. (2012). Spectral color, synchrony, and extinction risk. *Theoretical Ecology*, *5*, 545–554. https://doi.org/10.1007/s12080-011-0145-x

Mann, M. E., Rahmstorf, S., Kornhuber, K., Steinman, B. A., Miller, S. K., & Coumou, D. (2017). Influence of anthropogenic climate change on planetary wave resonance and extreme weather events. *Scientific Reports*, *7*, 45242. https://doi.org/10.1038/srep45242

Miramontes, O., & Rohani, P. (2002). Estimating $1/f^{\alpha}$ scaling exponents from short time-series. *Physica D: Nonlinear Phenomena*, *166*, 147–154. https://doi.org/10.1016/S0167-2789(02)00429-3

Mitchell, T. D., & Jones, P. D. (2005). An improved method of constructing a database of monthly climate observations and associated high-resolution grids. *International Journal of Climatology*, *25*, 693–712. https://doi.org/10.1002/joc.1181

O'Connell, P. E., Koutsoyiannis, D., Lins, H. F., Markonis, Y., Montanari, A., & Cohn, T. (2016). The scientific legacy of Harold Edwin Hurst (1880–1978). *Hydrological Sciences Journal*, *61*, 1571–1590. https://doi.org/10.1080/02626667.2015.1125998

Peterman, R. M. (1990). Statistical power analysis can improve fisheries research and management. *Canadian Journal of Fisheries and Aquatic Sciences*, *47*, 2–15. https://doi.org/10.1139/f90-001

Pimm, S. L., & Redfearn, A. (1988). The variability of population densities. *Nature*, *334*, 613–614. https://doi.org/10.1038/334613a0

Post, E., & Forchhammer, M. C. (2002). Synchronization of animal population dynamics by large-scale climate. *Nature*, *420*, 168–171. https://doi.org/10.1038/nature01064

Power, S., Delage, F., Chung, C., Kociuba, G., & Keay, K. (2013). Robust twenty-first-century projections of El Niño and related precipitation variability. *Nature*, *502*, 541–545.

Ripa, J., & Heino, M. (1999). Linear analysis solves two puzzles in population dynamics: The route to extinction and extinction in coloured environments. *Ecology Letters*, *2*, 219–222. https://doi.org/10.1046/j.1461-0248.1999.00073.x

Ripa, J., & Ives, A. R. (2003). Food web dynamics in correlated and autocorrelated environments. *Theoretical Population Biology*, *64*, 369–384. https://doi.org/10.1016/S0040-5809(03)00089-3

Rohani, P., Miramontes, O., & Keeling, M. J. (2004). The colour of noise in short ecological time series data. *Mathematical Medicine and Biology: A Journal of the IMA*, *21*, 63–72. https://doi.org/10.1093/imammb/21.1.63

Roughgarden, J. (1975). A simple model for population dynamics in stochastic environments. *The American Naturalist*, *109*, 713–736. https://doi.org/10.1086/283039

Royama, T. (1981). Fundamental concepts and methodology for the analysis of animal population dynamics, with particular reference to univoltine species. *Ecological Monographs*, *51*, 473–493. https://doi.org/10.2307/2937325

Ruokolainen, L., Fowler, M. S., & Ranta, E. (2007). Extinctions in competitive communities forced by coloured environmental variation. *Oikos*, *116*, 439–448. https://doi.org/10.1111/j.2006.0030-1299.15586.x

Ruokolainen, L., Lindén, A., Kaitala, V., & Fowler, M. S. (2009). Ecological and evolutionary dynamics under coloured environmental variation. *Trends in Ecology and Evolution*, *24*, 555–563.

Ruokolainen, L., Ranta, E., Kaitala, V., & Fowler, M. S. (2009). Community stability under different correlation structures of species' environmental responses. *Journal of Theoretical Biology*, *261*, 379–387.

Ruokolainen, L., & Fowler, M. S. (2008). Community extinction patterns in coloured environments. *Proceedings of the Royal Society B: Biological Sciences*, *275*, 1775–1783.

Rybski, D., Bunde, A., Havlin, S., & vonStorch, H. (2006). Long-term persistence in climate and the detection problem. *Geophysical Research Letters*, *33*, L06718.

Sabo, J. L., & Post, D. M. (2008). Quantifying periodic, stochastic and catastrophic environmental variation. *Ecological Monographs*, *78*, 19–40. https://doi.org/10.1890/06-1340.1

Schwager, M., Johst, K., & Jeltsch, F. (2006). Does red noise increase or decrease extinction risk? Single extreme events versus series of unfavorable conditions. *The American Naturalist*, *167*, 879–888. https://doi.org/10.1086/503609

Steele, J. H. (1985). A comparison of terrestrial and marine ecological systems. *Nature*, *313*, 355–358. https://doi.org/10.1038/313355a0

Stumpf, M. P. H., & Porter, M. A. (2012). Critical truths about power laws. *Science*, *335*, 665–666. https://doi.org/10.1126/science.1216142

The global population dynamics database. (1999). NERC Centre for Population Biology, Imperial College London. https://www.imperial.ac.uk/cpb/gpdd2/

Thomas, L. (1997). Retrospective power analysis. *Conservation Biology*, *11*, 276–280. https://doi.org/10.1046/j.1523-1739.1997.96102.x

van de Pol, M., Vindenes, Y., Sæther, B.-E., Engen, S., Ens, B. J., Oosterbeek, K., & Tinbergen, J. M. (2011). Poor environmental tracking can make extinction risk insensitive to the colour of environmental noise. *Proceedings of the Royal Society B: Biological Sciences*, *278*, 3713–3722.

Vasseur, D. A., & Yodzis, P. (2004). The color of environmental noise. *Ecology*, *85*, 1146–1152. https://doi.org/10.1890/02-3122

Wigley, T. M. L., Smith, R. L., & Santer, B. D. (1998). Anthropogenic influence on the autocorrelation structure of hemispheric-mean temperatures. *Science*, *282*, 1676–1679.

BIOSKETCH

David Gilljam is an ecologist with a background in computer engineering, whose research focus lies on the effects of environmental variation and within- and between-species interactions on the dynamics, stability and functioning of ecological networks.

Mike S. Fowler is interested in understanding how interactions among species and the environment shape the fluctuations we observe in population and community dynamics in ecosystems.

SUPPORTING INFORMATION

Additional supporting information may be found online in the Supporting Information section at the end of the article.

Figure S1.1. Distributions of model evidence ratios.

Figure S1.2. Scatterplots of colour coefficients of environmental time-series estimated from the frequency and time-domains.

Figure S1.3. Proportions of coloured or white environmental covariates associated with animal classes.

Figure S1.4. Number of points (years) needed to detect a specific colour parameter.

Table S1. Statistics from the 163 short and 160 long environmental time-series analysed in the study.

Figure S2.1. Estimated colour coefficients from environmental variables, using detrended and undetrended time-series data.

Figure S3.1. The MSM performed on an example artificial time-series.

Figure S3.2. Comparison of the MSM and the normal FFT method for estimating colour coefficients in the frequency-domain

How to cite this article: Gilljam D, Knape J, Lindén A, Mugabo M, Sait SM, Fowler MS. The colour of environmental fluctuations associated with terrestrial animal population dynamics. *Global Ecol Biogeogr.* 2018;00:1–13. https://doi.org/10.1111/geb.12824